Superweakly interacting massive particle dark matter signals from the early Universe

Jonathan L. Feng, Arvind Rajaraman, and Fumihiro Takayama
Department of Physics and Astronomy, University of California, Irvine, California 92697, USA
(Received 10 June 2003; published 12 September 2003)

Cold dark matter may be made of superweakly interacting massive particles, super-WIMP's, that naturally inherit the desired relic density from late decays of metastable WIMP's. Well-motivated examples are weak-scale gravitinos in supergravity and Kaluza-Klein gravitons from extra dimensions. These particles are impossible to detect in all dark matter experiments. We find, however, that super-WIMP dark matter may be discovered through cosmological signatures from the early Universe. In particular, super-WIMP dark matter has observable consequences for big bang nucleosynthesis and the cosmic microwave background (CMB), and may explain the observed underabundance of ^{7}Li without upsetting the concordance between deuterium and CMB baryometers. We discuss the implications for future probes of CMB blackbody distortions and collider searches for new particles. In the course of this study, we also present a model-independent analysis of entropy production from late-decaying particles in light of Wilkinson microwave anisotropy probe data.

DOI: 10.1103/PhysRevD.68.063504 PACS number(s): 95.35.+d, 26.35.+c, 98.80.Cq, 98.80.Es

I. INTRODUCTION

Recently, we proposed that dark matter is made of superweakly interacting massive particles (super-WIMP's) [1]. This possibility is realized in well-studied frameworks for new particle physics, such as those with weak-scale supersymmetry or extra spacetime dimensions, and provides a qualitatively new possibility for nonbaryonic cold dark matter.

The basic idea is as follows. Taking the supersymmetric case for concreteness, consider models with high-scale supersymmetry breaking (supergravity models) and R-parity conservation. If the lightest supersymmetric particle (LSP) is the neutralino, with a mass and interaction cross section set by the weak scale $M_{\rm weak}\sim 100$ GeV–1 TeV, such models are well known to provide an excellent dark matter candidate, which naturally freezes out with the desired relic density [2,3].

This scenario relies on the (often implicit) assumption that the gravitino is heavier than the lightest standard model superpartner. However, even in simple and constrained supergravity models, such as minimal supergravity [4–7], the gravitino mass is known only to be of the order of $M_{\rm weak}$ and is otherwise unspecified. Given this uncertainty, assume that the LSP is not a standard model superpartner, but the gravitino. The lightest standard model superpartner is then the next-lightest supersymmetric particle (NLSP). If the Universe is reheated to a temperature below $\sim 10^{10}$ GeV after inflation [8], the number of gravitinos is negligible after reheating. Then, because the gravitino couples only gravitationally with all interactions suppressed by the Planck scale $M_{\rm Pl}\simeq 1.2\times 10^{19}$ GeV, it plays no role in the thermodynamics of the early Universe. The NLSP therefore freezes out as usual; if it is weakly interacting, its relic density will again be near the desired value. However, much later, after

$$\tau\sim \frac{M_{\rm Pl}^2}{M_{\rm weak}^3}\sim 10^5\ {\rm s}\text{–}10^8\ {\rm s}, \tag{1}$$

the WIMP decays to the LSP, converting much of its energy density to gravitinos. Gravitino LSP's therefore form a significant relic component of our Universe, with a relic abundance naturally in the desired range near $\Omega_{\rm DM}\simeq 0.23$ [9]. Models with weak-scale extra dimensions also provide a similar dark matter particle in the form of Kaluza-Klein (KK) gravitons [1], with Kaluza-Klein gauge bosons or leptons playing the role of the WIMP [10]. As such dark matter candidates naturally preserve the WIMP relic abundance, but have interactions that are weaker than weak, we refer to the whole class of such particles as ''super-WIMP's.''

WIMP decays produce super-WIMP's and also release energy in standard model particles. It is important to check that such decays are not excluded by current constraints. The properties of these late decays are determined by what particle is the WIMP and two parameters: the WIMP and super-WIMP masses, $m_{\rm WIMP}$ and $m_{\rm SWIMP}$. Late-decaying particles in the early Universe cosmology have been considered in numerous studies [11–17]. For a range of natural weak-scale values of $m_{\rm WIMP}$ and $m_{\rm SWIMP}$, we found that WIMP $\rightarrow$SWIMP decays do not violate the most stringent existing constraints from big bang nucleosynthesis (BBN) and the cosmic microwave background (CMB) [1]. Super-WIMP dark matter therefore provides a new and viable dark matter possibility in some of the leading candidate frameworks for new physics.

Super-WIMP dark matter differs markedly from other known candidates with only gravitational interactions. Previous examples include $\sim$keV gravitinos [18], which form warm dark matter. The masses of such gravitinos are determined by a new scale intermediate between the weak and Planck scales at which supersymmetry is broken. Superheavy candidates have also been proposed, where the dark matter candidate's mass is itself at some intermediate scale between the weak and Planck scales, as in the case of wimpzillas [19]. In these and other scenarios [20], the dark matter abundance is dominantly generated by gravitational interactions at very large temperatures. In contrast to these, the properties of super-WIMP dark matter are determined by only the known mass scales $M_{\rm weak}$ and $M_{\rm Pl}$. Super-WIMP dark matter is therefore found in minimal extensions of the

standard model, and super-WIMP scenarios are therefore highly predictive, and, as we shall see, testable. In addition, super-WIMP dark matter inherits its relic density from WIMP thermal relic abundances, and so is in the desired range. Super-WIMP dark matter therefore preserves the main quantitative virtue of conventional WIMP's, naturally connecting the electroweak scale to the observed relic density.

Here we explore the signals of super-WIMP dark matter. Because super-WIMP's have interactions suppressed by $M_{\rm Pl}$, one might expect that they are impossible to detect. In fact, they are impossible to detect in all conventional direct and indirect dark matter searches. However, we find signatures through probes of the early Universe. Although the super-WIMP dark matter scenario passes present constraints, BBN and CMB observations do exclude some of the *a priori* interesting parameter space with $m_{\rm WIMP}, m_{\rm SWIMP} \sim M_{\rm weak}$. There may therefore be observable consequences for parameters near the boundary of the excluded region. Certainly, given expected future advances in the precision of BBN and CMB data, some super-WIMP dark matter scenarios imply testable predictions for upcoming observations.

Even more tantalizing, present data may already show evidence for this scenario. Late decays of WIMP's to super-WIMP's occur between the times of BBN and decoupling. They may therefore alter the inferred values of baryon density from BBN and CMB measurements by (1) destroying and creating light elements or (2) creating entropy [21]. We find that the second effect is negligible, but the first may be significant. At present, the most serious disagreement between observed and predicted light element abundances is in ^{7}Li, which is underabundant in all precise observations to date. As we will show below, the super-WIMP scenario naturally predicts WIMP decay times and electromagnetic energy releases within an order of magnitude of $\tau \approx 3\times 10^6$ s and $\zeta_{\rm EM} \equiv \varepsilon_{\rm EM} Y_{\rm WIMP} \approx 10^{-9}$ GeV, respectively. This unique combination of values results in the destruction of ^{7}Li without disrupting the remarkable agreement between deuterium and CMB baryon density determinations [17].

We then discuss what additional implications the super-WIMP scenario may have for cosmology and particle physics. For cosmology, we find that, if ^{7}Li is in fact being destroyed by WIMP decays, bounds on μ distortions of the Planckian CMB spectrum are already near the required sensitivity, and future improvements may provide evidence for late decays to super-WIMP's. For particle physics, the super-WIMP explanation of dark matter favors certain WIMP and super-WIMP masses, and we discuss these implications.

II. SUPER-WIMP PROPERTIES

As outlined above, super-WIMP dark matter is produced in decays WIMP$\rightarrow$SWIMP$+S$, where S denotes one or more standard model particles. The super-WIMP is essentially invisible, and so the observable consequences rely on finding signals of S production in the early Universe. In principle, the strength of these signals depends on what S is and its initial energy distribution. For the parameters of greatest interest here, however, S quickly initiates electromagnetic or hadronic cascades. As a result, the observable consequences depend only on the WIMP's lifetime τ and the average total electromagnetic or hadronic energy released in the WIMP decay [11–17,22].

We will determine τ as a function of the two relevant free parameters $m_{\rm WIMP}$ and $m_{\rm SWIMP}$ for various WIMP candidates. These calculations are, of course, in agreement with the estimate of Eq. (1), and so WIMP's decay on time scales of the order of 1 y, when the Universe is radiation-dominated and only neutrinos and photons are relativistic. In terms of τ, WIMP's decay at redshift

$$z \simeq 4.9\times 10^6 \left[\frac{10^6\ {\rm s}}{\tau}\right]^{1/2} \tag{2}$$

and temperature

$$T = \left[\frac{90 M_*^2}{4\pi^2 \tau^2 g_*(T)}\right]^{1/4} \simeq 0.94\ {\rm keV}\left[\frac{10^6\ {\rm s}}{\tau}\right]^{1/2}, \tag{3}$$

where $M_* = M_{\rm Pl}/\sqrt{8\pi} \simeq 2.4\times 10^{18}$ GeV is the reduced Planck mass, and $g_*(T) = 29/4$ is the effective number of relativistic degrees of freedom during WIMP decay.

The electromagnetic energy release is conveniently written in terms of

$$\zeta_{\rm EM} \equiv \varepsilon_{\rm EM} Y_{\rm WIMP}, \tag{4}$$

where $\varepsilon_{\rm EM}$ is the initial electromagnetic energy released in each WIMP decay, and $Y_{\rm WIMP} \equiv n_{\rm WIMP}/n_\gamma^{\rm BG}$ is the number density of WIMP's before they decay, normalized to the number density of background photons $n_\gamma^{\rm BG} = 2\zeta(3)T^3/\pi^2$. We define hadronic energy release similarly as $\zeta_{\rm had} \equiv \varepsilon_{\rm had} Y_{\rm WIMP}$. In the super-WIMP scenario, WIMP velocities are negligible when they decay. We will be concerned mainly with the case where S is a single nearly massless particle, and so we define

$$E_S \equiv \frac{m_{\rm WIMP}^2 - m_{\rm SWIMP}^2}{2 m_{\rm WIMP}}, \tag{5}$$

the potentially visible energy in such cases. We will determine what fraction of E_S appears as electromagnetic energy $\varepsilon_{\rm EM}$ and hadronic energy $\varepsilon_{\rm had}$ in various scenarios below. For $Y_{\rm WIMP}$, each WIMP decay produces one super-WIMP, and so the WIMP abundance may be expressed in terms of the present super-WIMP abundance through

$$Y_{\rm WIMP} = Y_{{\rm SWIMP},\tau} = Y_{{\rm SWIMP},0} = \frac{\Omega_{\rm SWIMP}\rho_c}{m_{\rm SWIMP} n_{\gamma,0}^{\rm BG}}$$
$$\simeq 3.0\times 10^{-12}\left[\frac{\rm TeV}{m_{\rm SWIMP}}\right]\left[\frac{\Omega_{\rm SWIMP}}{0.23}\right]. \tag{6}$$

For $\varepsilon_{\rm EM} \sim E_S \sim m_{\rm SWIMP} \sim M_{\rm weak}$, Eqs. (5) and (6) imply that energy releases in the super-WIMP dark matter scenario are naturally of the order of

$$\zeta_{\rm EM} \sim 10^{-9}\ {\rm GeV}. \tag{7}$$

We now consider various possibilities, beginning with the supersymmetric framework and two of the favored supersymmetric WIMP candidates, neutralinos and charged sleptons. Following this, we consider WIMP's in extra dimensional scenarios.

A. Neutralino WIMP's

A general neutralino χ is a mixture of the neutral *B*-ino, *W*-ino, and Higgsinos. Writing $\chi = \mathbf{N}_{11}(-i\tilde{B}) + \mathbf{N}_{12}(-i\tilde{W}) + \mathbf{N}_{13}\tilde{H}_u + \mathbf{N}_{14}\tilde{H}_d$, we find the decay width

$$\Gamma(\chi \to \gamma\tilde{G}) = \frac{|\mathbf{N}_{11}|^2 \cos^2\theta_W + |\mathbf{N}_{12}|^2 \sin^2\theta_W}{48\pi M_*^2} \times \frac{m_\chi^5}{m_{\tilde{G}}^2}\left[1 - \frac{m_{\tilde{G}}^2}{m_\chi^2}\right]^3\left[1 + 3\frac{m_{\tilde{G}}^2}{m_\chi^2}\right]. \quad (8)$$

This decay width, and all those that follow, includes the contributions from couplings to both the spin $\pm 3/2$ and $\pm 1/2$ gravitino polarizations. These must all be included, as they are comparable in models with high-scale supersymmetry breaking.

There are also other decay modes. The two-body final states $Z\tilde{G}$ and $h\tilde{G}$ may be kinematically allowed, and three-body final states include $\ell\bar{\ell}\tilde{G}$ and $q\bar{q}\tilde{G}$. For the WIMP lifetimes we are considering, constraints on electromagnetic energy release from BBN are well-studied [14,15,17], but constraints on hadronic cascades are much less certain [22]. Below, we assume that electromagnetic cascades are the dominant constraint and provide a careful analysis of these bounds. If the hadronic constraint is strong enough to effectively exclude two-body decays leading to hadronic energy, our results below are strictly valid only for the case $\chi = \tilde{\gamma}$, where $\chi \to \gamma\tilde{G}$ is the only possible two-body decay. If the hadronic constraint is strong enough to exclude even three-body hadronic decays, such as $\tilde{\gamma} \to q\bar{q}\tilde{G}$, the entire neutralino super-WIMP scenario may be excluded, leaving only slepton super-WIMP scenarios (discussed below) as a viable possibility. Detailed studies of BBN constraints on hadronic cascades at $\tau \sim 10^6$ s may therefore have important implications for super-WIMP's.

With the above caveats in mind, we now focus on *B*-ino-like neutralinos, the lightest neutralinos in many simple supergravity models. For pure *B*-inos,

$$\Gamma(\tilde{B} \to \gamma\tilde{G}) = \frac{\cos^2\theta_W}{48\pi M_*^2}\frac{m_{\tilde{B}}^5}{m_{\tilde{G}}^2}\left[1 - \frac{m_{\tilde{G}}^2}{m_{\tilde{B}}^2}\right]^3\left[1 + 3\frac{m_{\tilde{G}}^2}{m_{\tilde{B}}^2}\right]. \quad (9)$$

In the limit $\Delta m \equiv m_{\rm WIMP} - m_{\rm SWIMP} \ll m_{\rm SWIMP}$, $\Gamma(\tilde{B} \to \gamma\tilde{G}) \propto (\Delta m)^3$ and the decay lifetime is

$$\tau(\tilde{B} \to \gamma\tilde{G}) \approx 2.3 \times 10^7 \ \text{s}\left[\frac{100\ \text{GeV}}{\Delta m}\right]^3, \quad (10)$$

independent of the overall $m_{\rm WIMP}$, $m_{\rm SWIMP}$ mass scale. This threshold behavior, sometimes misleadingly described as *P* wave, follows not from angular momentum conservation, but rather from the fact that the gravitino coupling is dimensional. For the case $S = \gamma$, clearly all of the initial photon energy is deposited in an electromagnetic shower, so

$$\varepsilon_{\rm EM} = E_\gamma, \quad \varepsilon_{\rm had} \simeq 0. \quad (11)$$

If the WIMP is a *B*-ino, given values of $m_{\rm WIMP}$ and $m_{\rm SWIMP}$, τ is determined by Eq. (9), and Eqs. (5) and (11) determine the energy release $\zeta_{\rm EM}$. These physical quantities are given in Fig. 1 for a range of $(m_{\rm SWIMP}, \Delta m)$.

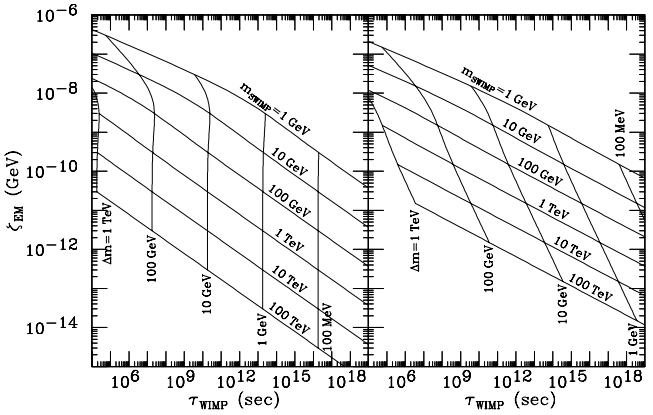

FIG. 1. Predicted values of the WIMP lifetime τ and electromagnetic energy release $\zeta_{\rm EM} \equiv \varepsilon_{\rm EM} Y_{\rm WIMP}$ in the $\tilde{B}$ (left) and $\tilde{\tau}$ (right) WIMP scenarios for $m_{\rm SWIMP} = 1$ GeV, 10 GeV, . . . , 100 TeV (top to bottom) and $\Delta m \equiv m_{\rm WIMP} - m_{\rm SWIMP} = 1$ TeV, 100 GeV, . . . , 100 MeV (left to right). For the $\tilde{\tau}$ WIMP scenario, we assume $\varepsilon_{\rm EM} = \frac{1}{2}E_\tau$.

B. Charged slepton WIMP's

For a slepton NLSP, the decay width is

$$\Gamma(\tilde{\ell} \to \ell\tilde{G}) = \frac{1}{48\pi M_*^2}\frac{m_{\tilde{\ell}}^5}{m_{\tilde{G}}^2}\left[1 - \frac{m_{\tilde{G}}^2}{m_{\tilde{\ell}}^2}\right]^4. \quad (12)$$

This expression is valid for any scalar superpartner decaying to a nearly massless standard model partner. In particular, it holds for $\tilde{\ell} = \tilde{e}$, $\tilde{\mu}$, or $\tilde{\tau}$, and arbitrary mixtures of the $\tilde{\ell}_L$ and $\tilde{\ell}_R$ gauge eigenstates. In the limit $\Delta m \equiv m_{\rm WIMP} - m_{\rm SWIMP} \ll m_{\rm SWIMP}$, the decay lifetime is

$$\tau(\tilde{\ell} \to \ell\tilde{G}) \approx 3.6 \times 10^8 \ \text{s}\left[\frac{100\ \text{GeV}}{\Delta m}\right]^4 \frac{m_{\tilde{G}}}{1\ \text{TeV}}. \quad (13)$$

For selectrons, the daughter electron will immediately initiate an electromagnetic cascade, so

$$\varepsilon_{\rm EM} \simeq E_e, \quad \varepsilon_{\rm had} \simeq 0. \quad (14)$$

Smuons produce muons. For the muon energies $E_\mu \sim M_{\rm weak}$ and temperatures T_τ of interest, $E_\mu T_\tau \ll m_\mu^2$. These muons therefore interact with background photons through $\mu\gamma_{\rm BG} \to \mu\gamma$ with the Thomson cross section for muons. The interaction time is

$$\tau_{\rm int}=[\sigma v n_\gamma^{\rm BG}]^{-1}=\left[\left(\frac{8\pi\alpha^2}{3m_\mu^2}\right)\left(\frac{2\zeta(3)T_\tau^3}{\pi^2}\right)\right]^{-1}$$
$$\simeq 7\times 10^{-5}\ {\rm s}\left[\frac{\rm keV}{T_\tau}\right]^3. \quad (15)$$

This is typically shorter than the time-dilated muon decay time $(E_\mu/m_\mu)2.0\times 10^{-6}$ s. The muon energy is, therefore, primarily transferred to electromagnetic cascades, and so

$$\varepsilon_{\rm EM}\simeq E_\mu,\quad \varepsilon_{\rm had}=0. \quad (16)$$

If muons decay before interacting, some electromagnetic energy will be lost to neutrinos, but in any case, $\varepsilon_{\rm had}\approx 0$, and hadronic cascades may be safely ignored.

Finally, stau NLSP's decay to taus. Before interacting, these decay to e, μ, π^0, $\pi^\pm$, and ν decay products. All of the energy carried by e, μ, and π^0 becomes electromagnetic energy. Decays $\pi^+\to\mu^+\nu$ also initiate electromagnetic cascades with energy $\sim E_{\pi^+}/2$. Making the crude assumption that energy is divided equally among the τ decay products in each decay mode, and summing the e, μ, π^0, and half of the $\pi^\pm$ energies weighted by the appropriate branching ratios, we find that the minimum electromagnetic energy produced in τ decays is $\varepsilon_{\rm EM}^{\rm min}\approx\frac{1}{3}E_\tau$. The actual electromagnetic energy may be larger. For example, for charged pions, following the analysis for muons above, the interaction time for $\pi^\pm\gamma_{\rm BG}\to\pi^\pm\gamma$ is of the same order as the time-dilated decay time $(E_{\pi^\pm}/m_{\pi^\pm})2.6\times 10^{-8}$ s. Which process dominates depends on model parameters. Neutrinos may also initiate electromagnetic showers if the rate for $\nu\nu_{\rm BG}\to e^+e^-$ is significant relative to $\nu\nu_{\rm BG}\to\nu\nu$.

All of the τ decay products decay or interact electromagnetically before initiating hadronic cascades. The hadronic interaction time for pions and kaons is

$$\tau_{\rm int}^{\rm had}=[\sigma_{\rm had}v n_B]^{-1}=[\sigma_{\rm had}v\,\eta n_\gamma^{\rm BG}]^{-1} \quad (17)$$
$$\simeq 18\ {\rm s}\left[\frac{100\ {\rm mb}}{\sigma_{\rm had}v}\right]\left[\frac{6\times 10^{-10}}{\eta}\right]\left[\frac{\rm keV}{T_\tau}\right]^3, \quad (18)$$

where η is the baryon-to-photon ratio, and we have normalized the cross section to the largest possible value. We see that hadronic interactions are completely negligible, as there are very few nucleons with which to interact. In fact, the leading contribution to hadronic activity comes not from interactions with the existing baryons, but from decays to three-body and four-body final states, such as $\ell Z\tilde{G}$ and $\ell q\bar{q}\tilde{G}$, that may contribute to hadronic energy. However, the branching ratios for such decays are also extremely suppressed, with values $\sim 10^{-3}$–10^{-5} [23]. In contrast to the case for neutralinos, then, the constraints on electromagnetic energy release are guaranteed to be the most stringent, and constraints on hadronic energy release may be safely ignored for slepton WIMP scenarios.

Combining all of these results for stau NLSP's, we find that

$$\varepsilon_{\rm EM}\approx\tfrac{1}{3}E_\tau-E_\tau,\quad \varepsilon_{\rm had}=0, \quad (19)$$

where the range in $\varepsilon_{\rm EM}$ results from the possible variation in electromagnetic energy from $\pi^\pm$ and ν decay products. The precise value of $\varepsilon_{\rm EM}$ is in principle calculable once the stau's chirality and mass, and the super-WIMP mass, are specified. However, as the possible variation in $\varepsilon_{\rm EM}$ is not great relative to other effects, we will simply present results below for the representative value of $\varepsilon_{\rm EM}=\frac{1}{2}E_\tau$.

For slepton WIMP scenarios, Eq. (12) determines the WIMP lifetime τ in terms of $m_{\rm WIMP}$ and $m_{\rm SWIMP}$, and $\zeta_{\rm EM}$ is determined by Eq. (5) and either Eq. (14), (16), or (19). These physical quantities are given in Fig. 1 in the $\tilde{\tau}$ WIMP scenario for a range of $(m_{\rm WIMP},\Delta m)$. For natural weak-scale values of these parameters, the lifetimes and energy releases in the neutralino and stau scenarios are similar. A significant difference is that larger WIMP masses are typically required in the slepton scenario to achieve the required relic abundance. However, thermal relic densities rely on additional supersymmetry parameters, and such model-dependent analyses are beyond the scope of this work.

C. KK gauge boson and KK charged lepton WIMP's

In scenarios with TeV^{-1}-size universal extra dimensions, KK gravitons are super-WIMP candidates. The WIMP's that decay to graviton super-WIMP's then include the 1st level KK partners of gauge bosons and leptons.

For the KK gauge boson WIMP scenario, letting $V^1=B^1\cos\theta_W^1+W^1\sin\theta_W^1$,

$$\Gamma(V^1\to\gamma G^1)=\frac{\cos^2\theta_W\cos^2\theta_W^1+\sin^2\theta_W\sin^2\theta_W^1}{72\pi M_*^2}$$
$$\times\frac{m_{V^1}^7}{m_{G^1}^4}\left[1-\frac{m_{G^1}^2}{m_{V^1}^2}\right]^3\left[1+3\frac{m_{G^1}^2}{m_{V^1}^2}+6\frac{m_{G^1}^4}{m_{V^1}^4}\right]. \quad (20)$$

For a B^1-like WIMP, this reduces to

$$\Gamma(B^1\to\gamma G^1)=\frac{\cos^2\theta_W}{72\pi M_*^2}\frac{m_{B^1}^7}{m_{G^1}^4}\left[1-\frac{m_{G^1}^2}{m_{B^1}^2}\right]^3$$
$$\times\left[1+3\frac{m_{G^1}^2}{m_{B^1}^2}+6\frac{m_{G^1}^4}{m_{B^1}^4}\right]. \quad (21)$$

In the limit $\Delta m\equiv m_{\rm WIMP}-m_{\rm SWIMP}\ll m_{\rm SWIMP}$, the decay lifetime is

$$\tau(B^1\to\gamma G^1)\approx 1.4\times 10^7\ {\rm s}\left[\frac{100\ {\rm GeV}}{\Delta m}\right]^3, \quad (22)$$

independent of the overall $m_{\rm WIMP}$, $m_{\rm SWIMP}$ mass scale, as in the analogous supersymmetric case.

For KK leptons, we have

$$\Gamma(\ell^1 \to \ell G^1) = \frac{1}{48\pi M_*^2} \frac{m_{\ell^1}^7}{m_{G^1}^4} \left[1 - \frac{m_{G^1}^2}{m_{\ell^1}^2}\right]^4 \left[2 + 3\frac{m_{G^1}^2}{m_{\ell^1}^2}\right], \tag{23}$$

valid for any KK lepton (or any KK fermion decaying to a massless standard model particle, for that matter). In the limit $\Delta m \equiv m_{\rm WIMP} - m_{\rm SWIMP} \ll m_{\rm SWIMP}$, the decay lifetime is

$$\tau(\ell^1 \to \ell G^1) \approx 7.3 \times 10^7 \ {\rm s} \left[\frac{100\ {\rm GeV}}{\Delta m}\right]^4 \frac{m_{G^1}}{1\ {\rm TeV}}. \tag{24}$$

In all cases, the expressions for $\varepsilon_{\rm EM}$ and $\varepsilon_{\rm had}$ are identical to those in the analogous supersymmetric scenario.

KK graviton super-WIMP's are therefore qualitatively similar to gravitino super-WIMP's. The expressions for WIMP lifetimes and abundances are similar, differing numerically only by $\mathcal{O}(1)$ factors. We therefore concentrate on the supersymmetric scenarios in the rest of this paper, with the understanding that all results apply, with $\mathcal{O}(1)$ adjustments, to the case of universal extra dimensions. A more important difference is that the desired thermal relic density is generally achieved for higher mass WIMP's in extra dimensional scenarios that in the supersymmetric case.

III. BARYOMETRY

A. Standard BBN and CMB baryometry

Big bang nucleosynthesis predicts primordial light element abundances in terms of one free parameter, the baryon-to-photon ratio $\eta \equiv n_B/n_\gamma$. At present, the observed D, ^{4}He, ^{3}He, and ^{7}Li abundances may be accommodated for baryon-to-photon ratios in the range [24]

$$\eta_{10} \equiv \eta/10^{-10} = 2.6\text{–}6.2. \tag{25}$$

In light of the difficulty of making precise theoretical predictions and reducing (or even estimating) systematic uncertainties in the observations, this consistency is a well-known triumph of standard big bang cosmology.

At the same time, given recent and expected advances in precision cosmology, the standard BBN picture merits close scrutiny. Recently, BBN baryometry has been supplemented by CMB data, which alone yields $\eta_{10} = 6.1 \pm 0.4$ [9]. Observations of deuterium absorption features in spectra from high redshift quasars imply a primordial D fraction of D/H $= 2.78^{+0.44}_{-0.38} \times 10^{-5}$ [25]. Combined with standard BBN calculations [26], this yields $\eta_{10} = 5.9 \pm 0.5$. The remarkable agreement between CMB and D baryometers has two new implications for scenarios with late-decaying particles. First, assuming there is no fine-tuned cancellation of unrelated effects, it prohibits significant entropy production between the times of BBN and decoupling. In Sec. III, we will show that the entropy produced in super-WIMP decays is indeed negligible. Second, the CMB measurement supports determinations of η from D, already considered by many to be the most reliable BBN baryometer. It suggests that if D and another BBN baryometer disagree, the "problem" lies with the other light element abundance—either its systematic uncertainties have been underestimated, or its value is modified by new astrophysics or particle physics. Such disagreements may therefore provide specific evidence for late-decaying particles in general, and super-WIMP dark matter in particular. We address this possibility here.

In standard BBN, the baryon-to-photon ratio $\eta_{10} = 6.0 \pm 0.5$ favored by D and CMB observations predicts [26]

$$Y_p = 0.2478 \pm 0.0010 \tag{26}$$

$$^3{\rm He/H} = (1.03 \pm 0.06) \times 10^{-5} \tag{27}$$

$$^7{\rm Li/H} = 4.7^{+0.9}_{-0.8} \times 10^{-10} \tag{28}$$

at 95% confidence level (CL), where Y_p is the ^{4}He mass fraction. At present all ^{7}Li measurements are below the prediction of Eq. (28). The ^{7}Li fraction may be determined precisely in very low metallicity stars. Three independent studies find

$$^7{\rm Li/H} = 1.5^{+0.9}_{-0.5} \times 10^{-10} \quad (95\%\ \ {\rm CL})[27] \tag{29}$$

$$^7{\rm Li/H} = 1.72^{+0.28}_{-0.22} \times 10^{-10} \quad (1\sigma + {\rm sys})[28] \tag{30}$$

$$^7{\rm Li/H} = 1.23^{+0.68}_{-0.32} \times 10^{-10} \quad ({\rm stat} + {\rm sys}, 95\%\ \ {\rm CL})[29], \tag{31}$$

where depletion effects have been estimated and included in the last value. Within the published uncertainties, the observations are consistent with each other but inconsistent with Eq. (28), with central values lower than predicted by a factor of 3–4. ^{7}Li may be depleted from its primordial value by astrophysical effects, for example, by rotational mixing in stars that brings lithium to the core where it may be burned [30,31], but it is controversial whether this effect is large enough to reconcile observations with the BBN prediction [29].

The other light element abundances are in better agreement. For example, for ^{4}He, Olive, Skillman, and Steigman find $Y_p = 0.234 \pm 0.002$ [32], lower than Eq. (26), but the uncertainty here is only statistical. Y_p is relatively insensitive to η and a subsequent study of Izotov and Thuan finds the significantly higher range 0.244 ± 0.002 [33]. ^{3}He has recently been restricted to the range $^3{\rm He/H} < (1.1 \pm 0.2) \times 10^{-5}$ [34], consistent with the CMB + D prediction of Eq. (27). Given these considerations, we view disagreements in ^{4}He and ^{3}He to be absent or less worrisome than in ^{7}Li. This view is supported by the global analysis of Ref. [26], which, taking the "high" Y_p values of Izotov and Thuan, finds $\chi^2 = 23.2$ for 3 degrees of freedom, where χ^2 is completely dominated by the ^{7}Li discrepancy.

B. Super-WIMP's and the ^{7}Li underabundance

Given the overall success of BBN, the first implication for new physics is that it should not drastically alter any of the light element abundances. This requirement restricts the amount of energy released at various times in the history of the Universe. A recent analysis by Cyburt, Ellis, Fields, and Olive of electromagnetic cascades finds that the shaded re-

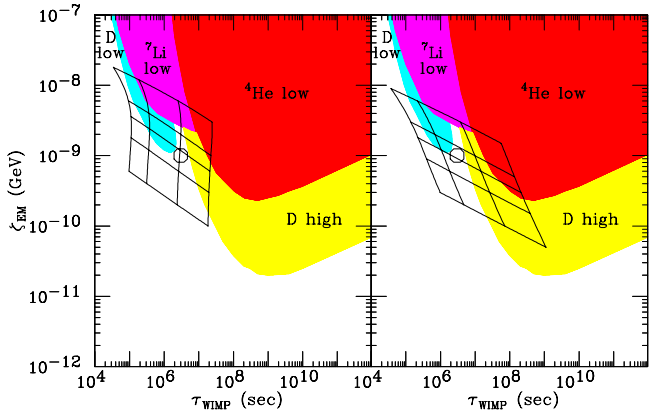

FIG. 2. The grid gives predicted values of the WIMP lifetime τ and electromagnetic energy release $\zeta_{\rm EM}\equiv\varepsilon_{\rm EM}Y_{\rm WIMP}$ in the $\tilde{B}$ (left) and $\tilde{\tau}$ (right) WIMP scenarios for $m_{\rm SWIMP}=100$ GeV, 300 GeV, 500 GeV, 1 TeV, and 3 TeV (top to bottom) and $\Delta m\equiv m_{\rm WIMP}-m_{\rm SWIMP}=600$ GeV, 400 GeV, 200 GeV, and 100 GeV (left to right). For the $\tilde{\tau}$ WIMP scenario, we assume $\varepsilon_{\rm EM}=\frac{1}{2}E_\tau$. The analysis of BBN constraints by Cyburt, Ellis, Fields, and Olive [17] excludes the shaded regions. The best fit region with $(\tau,\zeta_{\rm EM})\sim(3\times10^6\ {\rm s},10^{-9}\ {\rm GeV})$, where ^{7}Li is reduced to observed levels by late decays of WIMP's to super-WIMP's, is given by the circle.

gions of Fig. 2 are excluded by such considerations [17]. The various regions are disfavored by the following conservative criteria:

$$\text{D low:}\quad \mathrm{D/H}<1.3\times10^{-5} \tag{32}$$

$$\text{D high:}\quad \mathrm{D/H}>5.3\times10^{-5} \tag{33}$$

$$^4\text{He low:}\quad Y_p<0.227 \tag{34}$$

$$^7\text{Li low:}\quad {}^7\mathrm{Li/H}<0.9\times10^{-10}. \tag{35}$$

A subset of super-WIMP predictions from Fig. 1 is superimposed on this plot. The subset is for weak-scale $m_{\rm SWIMP}$ and Δm, the most natural values, given the independent motivations for new physics at the weak scale. As discussed previously [1], the BBN constraint eliminates some of the region predicted by the super-WIMP scenario, but regions with $m_{\rm WIMP},m_{\rm SWIMP}\sim M_{\rm weak}$ remain viable.

The ^{7}Li anomaly discussed above may be taken as evidence for new physics, however. To improve the agreement of observations and BBN predictions, it is necessary to destroy ^{7}Li without harming the concordance between CMB and other BBN determinations of η. This may be accomplished for $(\tau,\zeta_{\rm EM})\sim(3\times10^6\ {\rm s},10^{-9}\ {\rm GeV})$, as noted in Ref. [17]. This "best fit" point is marked in Fig. 2. The amount of energy release is determined by the requirement that ^{7}Li be reduced to observed levels without being completely destroyed—one cannot therefore be too far from the "^{7}Li low" region. In addition, one cannot destroy or create too much of the other elements. ^{4}He, with a binding threshold energy of 19.8 MeV, much higher than lithium's 2.5 MeV, is not significantly destroyed. On the other hand, D is loosely bound, with a binding energy of 2.2 MeV. The two primary reactions are D destruction through $\gamma{\rm D}\to np$ and D creation through $\gamma^4{\rm He}\to{\rm DD}$. These are balanced in the channel of Fig. 2 between the "low D" and "high D" regions, and the requirement that the electromagnetic energy that destroys ^{7}Li not disturb the D abundance specifies the preferred decay time $\tau\sim3\times10^6$ s.

Without theoretical guidance, this scenario for resolving the ^{7}Li abundance is rather fine-tuned: possible decay times and energy releases span tens of orders of magnitude, and there is no motivation for the specific range of parameters required to resolve BBN discrepancies. In the super-WIMP scenario, however, both τ and $\zeta_{\rm EM}$ are specified: the decay time is necessarily that of a gravitational decay of a weak-scale mass particle, leading to Eq. (1), and the energy release is determined by the requirement that super-WIMP's be the dark matter, leading to Eq. (7). Remarkably, these values coincide with the best fit values for τ and $\zeta_{\rm EM}$. More quantitatively, we note that the grids of predictions for the $\tilde{B}$ and $\tilde{\tau}$ scenarios given in Fig. 2 cover the best fit region. Current discrepancies in BBN light element abundances may therefore be naturally explained by super-WIMP dark matter.

This tentative evidence may be reinforced or disfavored in a number of ways. Improvements in the BBN observations discussed above may show if the ^{7}Li abundance is truly below predictions. In addition, measurements of ^{6}Li/H and ^{6}Li/^{7}Li may constrain astrophysical depletion of ^{7}Li and may also provide additional evidence for late decaying particles in the best fit region [14,15,17,35]. Finally, if the best fit region is indeed realized by WIMP$\to$SWIMP decays, there are a number of other testable implications for cosmology and particle physics. We discuss these in Secs. IV and V.

IV. ENTROPY PRODUCTION

In principle, there is no reason for the BBN and CMB determinations of η to agree—they measure the same quantity, but at different epochs in the Universe's history, and η may vary [21]. What is expected to be constant is the number of baryons

$$N_B=n_BR^3=\eta n_\gamma^{\rm BG}R^3=\eta\frac{2\zeta(3)}{\pi^2}T^3R^3, \tag{36}$$

where R is the scale factor of the Universe. Since the entropy S is proportional to T^3R^3 when g_{*s}, the number of relativistic degrees of freedom for entropy, is constant,

$$\frac{\eta_f}{\eta_i}=\frac{S_i}{S_f}, \tag{37}$$

where the superscripts and subscripts i and f denote quantities at times t_i and t_f, respectively. The quantities η_i and η_f therefore must agree only if there is no entropy production between times t_i and t_f.

Conversely, as noted in Sec. II, the agreement of CMB and D baryometers implies that there cannot be large entropy generation in the intervening times [21], barring fine-tuned cancellations between this and other effects. WIMP decays

occur between BBN and decoupling and produce entropy. In this section, we show that, for energy releases allowed by the BBN constraints discussed above, the entropy generation has a negligible effect on baryometry.

We would like to determine the change in entropy from BBN at time t_i to decoupling at time t_f. The differential change in entropy in a comoving volume at temperature T is

$$dS = \frac{dQ}{T}, \tag{38}$$

where the differential energy injected into radiation is

$$dQ = \varepsilon_{\rm EM} n_{\rm WIMP} R^3 \frac{dt}{\tau}. \tag{39}$$

In Eq. (39), $n_{\rm WIMP}$ is the WIMP number density per comoving volume. R may be eliminated using

$$S = \frac{2\pi^2}{45} g_{*s} T^3 R^3. \tag{40}$$

Substituting Eqs. (39) and (40) into Eq. (38) and integrating, we find

$$\frac{S_f}{S_i} = \exp\left[\int_{t_i}^{t_f} \varepsilon_{\rm EM} n_{\rm WIMP} \frac{45}{2\pi^2 g_{*s}} \frac{1}{T^4} \frac{dt}{\tau} \right]. \tag{41}$$

As WIMP's decay, their number density is

$$n_{\rm WIMP} = n^i_{\rm WIMP} \frac{R_i^3}{R^3} e^{-t/\tau} = n^i_{\rm WIMP} \frac{g_{*s} S_i T^3}{g^i_{*s} S T_i^3} e^{-t/\tau}, \tag{42}$$

and so

$$\frac{S_f}{S_i} = \exp\left[\varepsilon_{\rm EM} n^i_{\rm WIMP} \frac{45}{2\pi^2 g^i_{*s}} \frac{1}{T_i^4} \int_{t_i}^{t_f} \frac{S_i T_i}{S T} e^{-t/\tau} \frac{dt}{\tau} \right]. \tag{43}$$

Equation (43) is always valid. However, it is particularly useful if the change in entropy may be treated as a perturbation, with $\Delta S \ll S_i$. Given the high level of consistency of η measurements from deuterium and the CMB, this is now a perfectly reasonable assumption. We may therefore solve Eq. (43) iteratively. In fact, the first approximate solution, obtained by setting $S_i/S = 1$ in the integral, is already quite accurate. The integral may be further simplified if the Universe is always radiation dominated between BBN and decoupling. This is certainly true in the present analysis, as

$$\frac{\rho_{\rm WIMP}}{\rho_R} = m_{\rm WIMP} Y_{\rm WIMP} \frac{60\zeta(3)}{\pi^4 g_* T} = \left[\frac{m_{\rm WIMP} Y_{\rm WIMP}}{4.5 \times 10^{-6}\ {\rm GeV}} \right] \left[\frac{3.36}{g_*} \right] \left[\frac{1\ {\rm keV}}{T} \right] \ll 1. \tag{44}$$

WIMP's therefore decay before their matter density dominates the energy density of the Universe. We may then use the radiation-dominated era relations

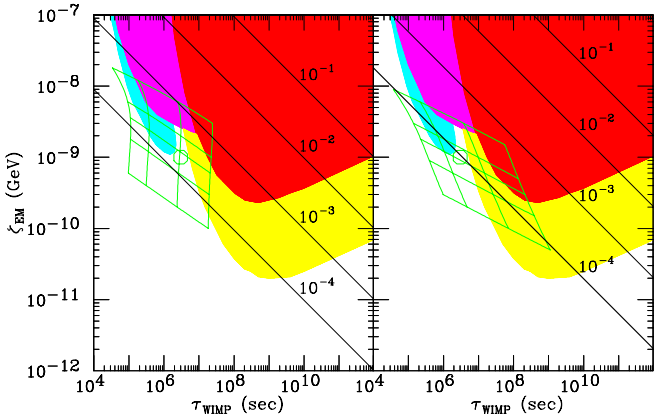

FIG. 3. Contours of fractional entropy production $\Delta S/S_i$ from late decays in the $(\tau, \zeta_{\rm EM})$ plane. Regions predicted by the super-WIMP dark matter scenario and BBN excluded and best fit regions are given as in Fig. 2.

$$t = \frac{1}{2H}, \quad H^2 = \frac{8\pi}{3M_{\rm Pl}^2} \rho_R, \quad \rho_R = \frac{\pi^2}{30} g_* T^4 \tag{45}$$

to eliminate T in favor of t in the integral of Eq. (43). Finally, $t_i \ll \tau \ll t_f$, and, as the dominant contribution to the integral is from $t \sim \tau$, we may replace g_* by g_*^τ, its (constant) value during the era of WIMP decay.

Exploiting all of these simplifications, the integral in Eq. (43) reduces to

$$\int_{t_i}^{t_f} \left(\frac{g_*}{g_*^i} \right)^{1/4} \left(\frac{t}{t_i} \right)^{1/2} e^{-t/\tau} \frac{dt}{\tau} \approx \left(\frac{g_*^\tau}{g_*^i} \right)^{1/4} \int_0^\infty \left(\frac{t}{t_i} \right)^{1/2} e^{-t/\tau} \frac{dt}{\tau} \tag{46}$$

$$= \frac{\sqrt{\pi}}{2} \left(\frac{g_*^\tau}{g_*^i} \right)^{1/4} \left(\frac{\tau}{t_i} \right)^{1/2}. \tag{47}$$

Finally, substituting Eq. (47) into Eq. (43) and again using the radiation-dominated era relations of Eq. (45), we find

$$\frac{S_f}{S_i} = \exp\left[\zeta(3) \frac{45^{3/4}}{\pi^{11/4}} \frac{(g_*^\tau)^{1/4}}{g^i_{*s}} \frac{\varepsilon_{\rm EM} n^i_{\rm WIMP}}{n^i_\gamma} \sqrt{\frac{\tau}{M_{\rm Pl}}} \right]. \tag{48}$$

For small entropy changes,

$$\frac{\Delta S}{S_i} \approx \ln \frac{S_f}{S_i} = 1.10 \times 10^{-4} \left[\frac{\zeta_{\rm EM}}{10^{-9}\ {\rm GeV}} \right] \left[\frac{\tau}{10^6\ {\rm s}} \right]^{1/2}, \tag{49}$$

where we have used $\zeta(3) \simeq 1.202$, and $g_*^\tau \simeq 3.36$ and $g^i_{*s} \simeq 3.91$ are the appropriate degrees of freedom, which include only the photon and neutrinos.

Contours of $\Delta S/S_i$ are given in the $(\tau, \zeta_{\rm EM})$ plane in Fig. 3 for late-decaying B-inos and staus. For reference, the BBN excluded and best fit regions are also repeated from Fig. 2, as are the regions predicted for natural super-WIMP scenarios. We find that the super-WIMP scenario naturally predicts $\Delta S/S_i \lesssim 10^{-3}$. Such deviations are beyond foreseeable sen-

sitivities in studies of CMB and BBN baryometry. Within achievable precisions, then, CMB and BBN baryometers may be directly compared to each other in super-WIMP dark matter discussions, as we have already done in Sec. II.

Entropy production at the percent level may be accessible in future baryometry studies. It is noteworthy, however, that, independent of theoretical framework, such large entropy production from electromagnetic energy release in late-decaying particles is excluded by BBN constraints for decay times $10^4\ \mathrm{s} < \tau < 10^{12}\ \mathrm{s}$. Only for decays very soon after BBN times $t_i \sim 1-100$ s or just before decoupling times $t_f \sim 10^{13}$ s can entropy production significantly distort the comparison between BBN and CMB baryon-to-photon ratios. In fact, only the very early decays are a viable source of entropy production, as very late time decays create unobserved CMB black body distortions, which we now discuss.

V. IMPLICATIONS FOR CMB BLACKBODY DISTORTIONS

The injection of electromagnetic energy may also distort the frequency dependence of the CMB blackbody radiation. For the decay times of interest, with redshifts $z \sim 10^5 - 10^7$, the resulting photons interact efficiently through $\gamma e^- \to \gamma e^-$, but photon number is conserved, since double Compton scattering $\gamma e^- \to \gamma\gamma e^-$ and thermal bremsstrahlung $eX \to eX\gamma$, where X is an ion, are inefficient. The spectrum therefore relaxes to statistical but not thermodynamic equilibrium, resulting in a Bose-Einstein distribution function

$$f_\gamma(E) = \frac{1}{e^{E/(kT)+\mu} - 1}, \tag{50}$$

with chemical potential $\mu \neq 0$.

For the low values of baryon density currently favored, the effects of double Compton scattering are more significant than those of thermal bremsstrahlung. The value of the chemical potential μ may therefore be approximated for small energy releases by the analytic expression [36]

$$\mu = 8.0\times 10^{-4}\left[\frac{\tau}{10^6\ \mathrm{s}}\right]^{1/2}\left[\frac{\zeta_{\mathrm{EM}}}{10^{-9}\ \mathrm{GeV}}\right] e^{-(\tau_{\mathrm{dC}}/\tau)^{5/4}}, \tag{51}$$

where

$$\tau_{\mathrm{dC}} = 6.1\times 10^6\ \mathrm{s}\left[\frac{T_0}{2.725\ \mathrm{K}}\right]^{-12/5}\left[\frac{\Omega_B h^2}{0.022}\right]^{4/5}\left[\frac{1-\frac{1}{2}Y_p}{0.88}\right]^{4/5}. \tag{52}$$

In Fig. 4 we show contours of chemical potential μ. The current bound is $\mu < 9\times 10^{-5}$ [24,37]. We see that, although there are at present no indications of deviations from black body, current limits are already sensitive to the super-WIMP scenario, and particularly to regions favored by the BBN considerations described in Sec. II. In the future, the diffuse microwave emission survey (DIMES) may improve sensitivities to $\mu \approx 2\times 10^{-6}$ [38]. The DIMES will therefore probe further into the super-WIMP parameter space, and will effectively probe all of the favored region where the ^{7}Li underabundance is explained by decays to super-WIMP's.

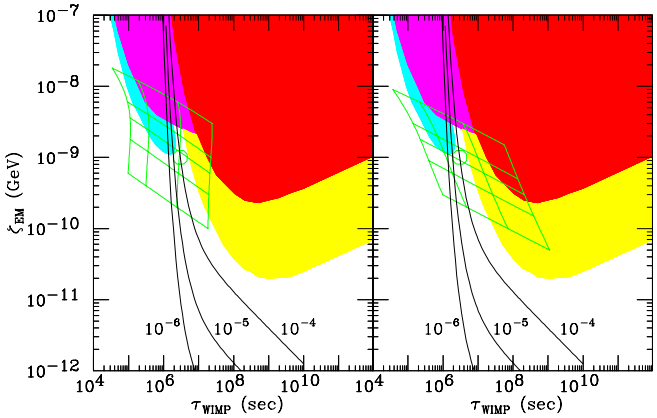

FIG. 4. Contours of μ, parametrizing the distortion of the CMB from a Planckian spectrum, in the $(\tau, \zeta_{\mathrm{EM}})$ plane. Regions predicted by the super-WIMP dark matter scenario, and BBN excluded and best fit regions are given as in Fig. 2.

VI. IMPLICATIONS FOR PARTICLE PHYSICS

The super-WIMP scenario has implications for the superpartner (and KK) spectrum, and for searches for supersymmetry (and extra dimensions) at particle physics experiments. In this section, we consider some of the implications for high energy colliders.

Lifetimes and energy releases are given as functions of m_{SWIMP} and Δm in Fig. 5. BBN and CMB baryometry, along with limits on CMB μ distortions, exclude some of this parameter space. The excluded regions were presented and discussed in Ref. [1].

Here we concentrate on the regions preferred by the tentative evidence for late decaying particles from BBN considerations. As noted above, the preferred lifetimes and energy releases for which ^{7}Li is reduced without sacrificing the concordance between CMB and D η determinations are a region around $(\tau, \zeta_{\mathrm{EM}}) \sim (3\times 10^6\ \mathrm{s}, 10^{-9}\ \mathrm{GeV})$. This region is

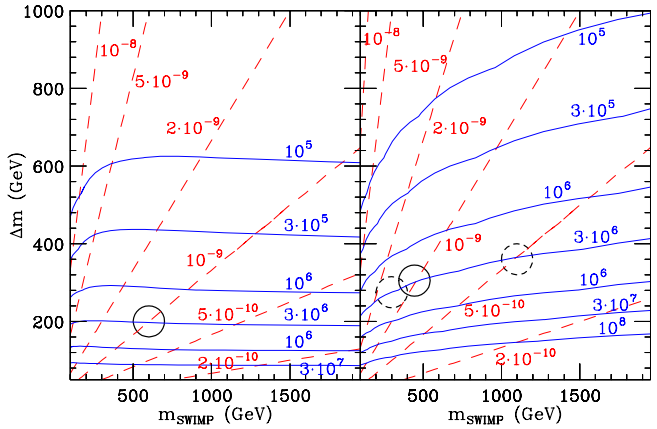

FIG. 5. Contours of constant τ (dashed, red) and constant $\zeta_{\mathrm{EM}} = \varepsilon_{\mathrm{EM}} Y_{\mathrm{WIMP}}$ (solid, blue) in the $(m_{\mathrm{SWIMP}}, \Delta m)$ plane in the $\tilde{B}$ (left) and $\tilde{\tau}$ (right) WIMP scenarios. The regions with BBN preferred values $(\tau, \zeta_{\mathrm{EM}}) \sim (3\times 10^6\ \mathrm{s}, 10^{-9}\ \mathrm{GeV})$ are given by the circles. For the $\tilde{\tau}$ WIMP scenario, the solid circle is favored if $\varepsilon_{\mathrm{EM}} = \frac{1}{2}E_\tau$; the dashed circles are favored if $\varepsilon_{\mathrm{EM}} = \frac{1}{3}E_\tau$ or $\varepsilon_{\mathrm{EM}} = E_\tau$.

highlighted in Fig. 5. For the $\tilde{\tau}$ case, we present a range of best fit regions to account for the possible range $\varepsilon_{\rm EM}=(\frac{1}{3}-1)E_\tau$ of Eq. (19) discussed in Sec. II.

Given some variation in the preferred values of τ and $\zeta_{\rm EM}$, there is a fair amount of variation in the underlying superpartner masses. We may draw some rough conclusions, however. For the $\tilde{B}$ WIMP scenario the preferred parameters are $m_{\tilde{G}}\sim 600$ GeV and $m_{\tilde{B}}\sim 800$ GeV. All other superpartners are necessarily heavier than $m_{\tilde{B}}$. The resulting superpartner spectrum is fairly heavy, although well within the reach of the Large Hadron Collider (LHC), assuming the remaining superpartners are not much heavier. This scenario will be indistinguishable at colliders from the usual supergravity scenario where the gravitino is heavier than the LSP and the usual signal of missing energy from neutralinos applies.

For the $\tilde{\tau}$ super-WIMP scenario, there are dramatic differences. From Fig. 5, the BBN preferred masses are $m_{\tilde{G}}\sim 300$–1100 GeV and $\Delta m=m_{\tilde{\tau}}-m_{\tilde{G}}\sim 300$–$400$ GeV. Although fairly heavy, this range of superpartner masses is again well within the reach of the LHC and possibly even future linear colliders. In this case, collider signatures contrast sharply with those of standard supergravity scenarios. Typically, the region of parameter space in which a stau is the lightest standard model superpartner is considered excluded by searches for charged dark matter. In the super-WIMP scenario, this region is allowed, as the stau is not stable, but metastable. Such particles therefore evade cosmological constraints, but are effectively stable on collider time scales. They appear as slow, highly ionizing charged tracks. This spectacular signal has been studied in the context of gauge-mediated supersymmetry breaking models with a relatively high supersymmetry-breaking scale [39], and discovery limits are, not surprisingly, much higher than in standard scenarios. It would be interesting to evaluate the prospects for discovering and studying meta-stable staus at the Tevatron, LHC, and future linear colliders in various super-WIMP scenarios.

VII. CONCLUSIONS AND FUTURE DIRECTIONS

Super-WIMP dark matter presents a qualitatively new dark matter possibility realized in some of the most promising frameworks for new physics. In supergravity, for example, super-WIMP dark matter is realized simply by assuming that the gravitino is the LSP. When the NLSP is a weakly interacting superpartner, the gravitino super-WIMP naturally inherits the desired dark matter relic density. The prime WIMP virtue connecting weak scale physics with the observed dark matter density is therefore preserved by super-WIMP dark matter.

Because super-WIMP dark matter interacts only gravitationally, searches for its effects in standard dark matter experiments are hopeless. At the same time, this superweak interaction implies that WIMP's decaying to it do so after BBN. BBN observations and later observations, such as of the CMB, therefore bracket the era of WIMP decays, and provide new signals. Super-WIMP and conventional WIMP dark matter therefore have disjoint sets of signatures, and we have explored the new opportunities presented by super-WIMP's in this study. We find that the super-WIMP scenario is not far beyond reach. In fact, precision cosmology already excludes some of the natural parameter space, and future improvements in BBN baryometry and probes of CMB μ distortions will extend this sensitivity.

We have also found that the decay times and energy releases generic in the super-WIMP scenario may naturally reduce ^{7}Li abundances to the observed levels without sacrificing the agreement between D and CMB baryometry. The currently observed ^{7}Li underabundance therefore provides evidence for the super-WIMP hypothesis. This scenario predicts that more precise BBN observations will expose a truly physical underabundance of ^{7}Li. In addition, probes of CMB μ distortions at the level of $\mu\sim 2\times 10^{-6}$ will be sensitive to the entire preferred region. An absence of such effects will exclude this explanation.

We have considered here the cases where neutralinos and sleptons decay to gravitinos and electromagnetic energy. In the case of selectrons, smuons, and staus, we have shown that BBN constraints on electromagnetic cascades provide the dominant bound. For neutralinos, however, the case is less clear. Neutralinos may produce hadronic energy through two-body decays $\chi\to Z\tilde{G},h\tilde{G}$, and three-body decays $\chi\to q\bar{q}\tilde{G}$. Detailed BBN studies constraining hadronic energy release may exclude such two-body decays, thereby limiting possible neutralino WIMP candidates to photinos, or even exclude three-body decays, thereby eliminating the neutralino WIMP scenario altogether. At present, detailed BBN studies of hadronic energy release incorporating the latest data are limited to decay times $\tau\lesssim 10^4$ s [22]. We strongly encourage detailed studies for later times $\tau\sim 10^6$ s, as these may have a great impact on what super-WIMP scenarios are viable.

Finally, in the course of this study, we presented a model-independent study of entropy production in light of the recent Wilkinson microwave anisotropy probe data. The agreement of precise CMB and D baryon-to-photon ratios limits entropy production in the time between BBN and decoupling. However, constraints on BBN light element abundances and CMB distortions already provide stringent bounds. We have compared these constraints here. We find that BBN abundances and CMB blackbody distortions largely eliminate the possibility of significant entropy production. For fractional entropy changes at the percent level, which may be visible through comparison of future BBN and CMB baryometers, these other constraints require the entropy production to take place before $\sim 10^4$ s, that is, in a narrow window not long after BBN.

ACKNOWLEDGMENTS

We are grateful to M. Kaplinghat, H. Murayama, and T. Smecker-Hane for enlightening conversations and thank E. Wright and M. Kamionkowski for bringing future CMB experiments to our attention.

[1] J.L. Feng, A. Rajaraman, and F. Takayama, Phys. Rev. Lett. **91**, 011302 (2003).
[2] H. Goldberg, Phys. Rev. Lett. **50**, 1419 (1983).
[3] J. Ellis, J.S. Hagelin, D.V. Nanopoulos, and M. Srednicki, Phys. Lett. **127B**, 233 (1983).
[4] A.H. Chamseddine, R. Arnowitt, and P. Nath, Phys. Rev. Lett. **49**, 970 (1982).
[5] R. Barbieri, S. Ferrara, and C.A. Savoy, Phys. Lett. **119B**, 343 (1982).
[6] L.J. Hall, J. Lykken, and S. Weinberg, Phys. Rev. D **27**, 2359 (1983).
[7] L. Alvarez-Gaume, J. Polchinski, and M.B. Wise, Nucl. Phys. **B221**, 495 (1983).
[8] T. Moroi, H. Murayama, and M. Yamaguchi, Phys. Lett. B **303**, 289 (1993); M. Bolz, A. Brandenburg, and W. Buchmuller, Nucl. Phys. **B606**, 518 (2001).
[9] D.N. Spergel *et al.*, astro-ph/0302209.
[10] G. Servant and T.M. Tait, Nucl. Phys. **B650**, 391 (2003); H.C. Cheng, J.L. Feng, and K.T. Matchev, Phys. Rev. Lett. **89**, 211301 (2002); G. Servant and T.M. Tait, New J. Phys. **4**, 99 (2002); D. Hooper and G.D. Kribs, Phys. Rev. D **67**, 055003 (2003); G. Bertone, G. Servant, and G. Sigl, *ibid.* **68**, 044008 (2003).
[11] J.R. Ellis, D.V. Nanopoulos, and S. Sarkar, Nucl. Phys. **B259**, 175 (1985).
[12] J.R. Ellis, G.B. Gelmini, J.L. Lopez, D.V. Nanopoulos, and S. Sarkar, Nucl. Phys. **B373**, 399 (1992).
[13] M. Kawasaki and T. Moroi, Astrophys. J. **452**, 506 (1995).
[14] E. Holtmann, M. Kawasaki, K. Kohri, and T. Moroi, Phys. Rev. D **60**, 023506 (1999).
[15] M. Kawasaki, K. Kohri, and T. Moroi, Phys. Rev. D **63**, 103502 (2001).
[16] T. Asaka, J. Hashiba, M. Kawasaki, and T. Yanagida, Phys. Rev. D **58**, 023507 (1998).
[17] R.H. Cyburt, J. Ellis, B.D. Fields, and K.A. Olive, Phys. Rev. D **67**, 103521 (2003).
[18] H. Pagels and J.R. Primack, Phys. Rev. Lett. **48**, 223 (1982); S. Weinberg, *ibid.* **48**, 1303 (1982); L.M. Krauss, Nucl. Phys. **B227**, 556 (1983); D.V. Nanopoulos, K.A. Olive, and M. Srednicki, Phys. Lett. **127B**, 30 (1983); M.Y. Khlopov and A.D. Linde, *ibid.* **138B**, 265 (1984); J.R. Ellis, J.E. Kim, and D.V. Nanopoulos, *ibid.* **145B**, 181 (1984); R. Juszkiewicz, J. Silk, and A. Stebbins, *ibid.* **158B**, 463 (1985).
[19] D.J. Chung, E.W. Kolb, and A. Riotto, Phys. Rev. Lett. **81**, 4048 (1998).
[20] See, e.g., V.S. Berezinsky, Phys. Lett. B **261**, 71 (1991).
[21] M. Kaplinghat and M.S. Turner, Phys. Rev. Lett. **86**, 385 (2001).
[22] M.H. Reno and D. Seckel, Phys. Rev. D **37**, 3441 (1988); S. Dimopoulos, R. Esmailzadeh, L.J. Hall, and G.D. Starkman, Nucl. Phys. **B311**, 699 (1989); K. Kohri, Phys. Rev. D **64**, 043515 (2001).
[23] J.L. Feng, A. Rajaraman, S. Su, and F. Takayama (unpublished).
[24] Particle Data Group, K. Hagiwara *et al.*, Phys. Rev. D **66**, 010001 (2002).
[25] D. Kirkman, D. Tytler, N. Suzuki, J.M. O'Meara, and D. Lubin, astro-ph/0302006.
[26] S. Burles, K.M. Nollett, and M.S. Turner, Astrophys. J. Lett. **552**, L1 (2001).
[27] J.A. Thorburn, Astrophys. J. **421**, 318 (1994).
[28] P. Bonifacio and P. Molaro, Mon. Not. R. Astron. Soc. **285**, 847 (1997).
[29] S.G. Ryan, T.C. Beers, K.A. Olive, B.D. Fields, and J.E. Norris, Astrophys. J. Lett. **530**, L57 (2000).
[30] M.H. Pinsonneault, T.P. Walker, G. Steigman, and V.K. Narayanan, Astrophys. J. **527**, 180 (1999).
[31] S. Vauclair and C. Charbonnel, Astrophys. J. **502**, 372 (1998).
[32] K.A. Olive, E. Skillman, and G. Steigman, Astrophys. J. **483**, 788 (1997).
[33] Y.I. Izotov and T.X. Thuan, Astrophys. J. **500**, 188 (1998).
[34] T.M. Bania, R.T. Rood, and D.S. Balser, Nature (London) **415**, 54 (2002).
[35] K. Jedamzik, Phys. Rev. Lett. **84**, 3248 (2000).
[36] W. Hu and J. Silk, Phys. Rev. Lett. **70**, 2661 (1993).
[37] D.J. Fixsen *et al.*, Astrophys. J. **473**, 576 (1996).
[38] See http://map.gsfc.nasa.gov/DIMES
[39] J.L. Feng and T. Moroi, Phys. Rev. D **58**, 035001 (1998).